WIDTH DEFORMATION OF THERMOPLASTIC PREPREG TAPES DURING AUTOMATED FIBER PLACEMENT

Sovit Agarwal[1,*], Daniël Peeters[2], Dominik Delisle[1] and Daniel Stefaniak[1,2]

[1]Institute of Lightweight Systems, Production Technologies, German Aerospace Center (DLR), Ottenbecker Damm 12, 21684 Stade, Germany
[2]Faculty of Aerospace Engineering, Delft University of Technology, 2629HS, Delft, The Netherlands
[*]Corresponding author. E-mail: sovit.agarwal@dlr.de

Keywords: Automated Fiber Placement (AFP), Gaps and Overlaps, Width deformation, Thermoplastic prepreg manufacturing, Humm3® Xenon Flashlamp

Abstract
In-situ Automated Fiber Placement (AFP) manufacturing of thermoplastic prepreg tapes has the potential to provide a fast and cost-effective manufacturing solution for large composite structures. However, it is prone to several defects, especially gaps and overlaps. One of the primary causes for this is the tape width deformation during placement. Current literature is not enough to understand this mechanism completely and the conventionally considered tape width deformation mechanism i.e., transverse squeeze flow has been suggested to be incorrect for AFP. Therefore, the research objective was to experimentally investigate the width deformation mechanism and the influence of processing parameters for thermoplastic prepreg tapes using humm3® as the heating device. The results show that the tape width deformation takes place both in the heating and consolidation phase of the process and involves spreading of the fiber-resin mixture. Additionally, the conformable roller has an influence on the post-processed tape cross-section profile. The surface roughness and the influence of the processing parameters indicate the role of temperature distribution as the influencing factor. Therefore, these results can be used to accurately model the tape width deformation to mitigate the problem of gaps and overlaps.

1. Introduction

AFP is a commonly used automated technique to manufacture typical aerospace structures. The fiber placement head consists of a heating device to heat the incoming material before it is placed on the tool and a compaction roller is used to apply pressure and conform the placed tape to the tool or the previously placed laminate called the substrate. The AFP process can be divided into three phases as illustrated in **Figure 1**. The heating phase is where the incoming tape and the substrate/tool is heated to the processing temperature, consolidation phase is where the bonding of the tape to the substrate takes place under the compaction roller and finally, solidification phase is where the tape and the substrate have been bonded and are cooled down to room temperature.

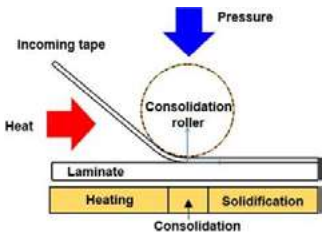

Figure 1. AFP processing phases of thermoplastic prepregs [1].

In-situ AFP processing i.e., processing without requiring a secondary step in the autoclave/oven is possible with thermoplastic prepreg tapes due to the absence of chemical cross-linking (in the case of

thermoset material) for consolidation. However, this technology is in its development phase as it is still prone to several defect formations during manufacturing, especially gaps and overlaps which is a major one and leads to several other defects [2]. One of the primary causes for these gaps and overlaps is the tape width deformation during placement and it becomes very crucial for in-situ AFP manufacturing as there is no secondary autoclave processing step that might alleviate it by the flow of the fiber-resin mixture under uniform heat and pressure.

Current literature on tape width deformation shows that the resulting tape width is influenced by processing parameters such as temperature, pressure and placement speed [3] [4] [5]. However, results from different studies do not agree with each other, indicating that the tape temperature distribution might be at play [3]. Additionally, the conventionally considered tape width deformation mechanism, namely transverse squeeze flow has been suggested to be incorrect for the AFP process as the experimental deformations do not agree with the results of the transverse squeeze flow model [3]. Clearly, the knowledge on this topic is lacking and additional research is required to mitigate the problem of gaps and overlaps due to tape width deformation.

Therefore, this study experimentally investigates the tape width deformation mechanism and the influence of processing parameters for thermoplastic prepreg tapes using in-situ AFP manufacturing with a xenon flashlamp as the heating device. The specimens were manufactured according to a full-factorial Design of Experiments (DoE) with heated length, nip-point temperature and compaction force as the variables. The tape width was measured for all the specimens to investigate the influence of these processing parameters and some post-processing analyses i.e., width measurement in the heating phase of the process, surface roughness analysis, tape cross-section profile and edge inspection were conducted to understand the tape width deformation mechanism.

2. Experimentation

2.1. Fiber Placement System and Specimen Manufacturing

The specimens were manufactured on a development AFP head, mounted on a KUKA 500 robot at the German Aerospace Center (DLR) in Stade, Germany. The machine was capable of processing quarter-inch thermoplastic prepreg tapes and laying up to 16 tapes simultaneously. However, for this study, only one tape was laid at a time to avoid any interaction effects between the tapes. The machine was equipped with a 130 mm wide broadband ($\lambda \simeq 200$ nm $-$ 1050 nm) Xenon flashlamp system humm3® from Heraeus Noblelight Ltd. Cambridge. The maximum input power for the flashlamp was 14 kW with an estimated input to output power efficiency of 0.5. A triangular-end shaped light guide with the two edges having different lengths and angles was used. A conformable silicone roller with a diameter of 85 mm and 60 shore hardness, wrapped in a thin layer of Teflon heat protective foil was used for the in-situ compaction of the specimens. The tool used for the specimen manufacturing was heated to 80 °C and covered with thin polyimide Upilex® film for easy release. The material used for this study was Toray Cetex® TC1225 (T700G Carbon, Semi-crystalline LM-PAEK, 194 gsm fiber areal weight, 34% resin content) in the form of 0.25" (6.35 mm) wide UD prepreg tapes.

Table 1. Process parameters used in the experimental study.

Heated length	Compaction force (N)	Nip-point temperature (°C)
Short (35-40 mm)	300	370
Long (45-50 mm)	900	420
		250*
		300*

The processing parameters for the experiments were determined based on relevance to in-situ AFP manufacturing. The only limitation in the used set-up was the power limitation of the humm3® flashlamp which would directly pose a limitation on the highest nip-point temperature achievable during the process. Therefore, a constant placement speed of 850 mm/min was used for all the specimens which

was slow enough to reach the desired highest temperature of 420 °C. A full factorial DoE as given in **Table 1** was selected for the study. For the temperature at nip-point, two temperatures were selected based on the typical processing temperature range and suggested nip-point temperature range for in-situ AFP processing by the material manufacturer. Additionally, a few extra specimens (marked with a * in **Table 1**) were added. Three samples of length 580 mm for each configuration of process parameters were manufactured.

2.2. Process Parameter Settings and Measurement

2.2.1. Compaction pressure

The compaction pressure for in-situ consolidation of the tape was varied by changing the force applied by the AFP head. To estimate the compaction pressure, ink imprints from the roller were used to measure the contact area under a range of forces applied by the AFP head statically as the effect of roller rotation on the normal pressure is negligible and therefore the dynamic pressure applied during the process can be simplified to a static one [6]. This method however, is only an approximation as it is assumed that the pressure distribution remains uniform for the entire contact area.

The average pressure values achieved for this study were 298 kPa for the 300 N specimens and 543 kPa for the 900 N specimens with (260, 325) and (515, 561) kPa as the minimum and maximum variation values recorded along the specimen course length respectively. The reason for this pressure variation is believed to be because of the roller not being completely balanced with respect to the axle and the layup tool not being completely flat.

2.2.2. Temperature

The nip-point temperature was varied by changing the pulse energy (voltage) and thereby the power (kW) of the broadband radiation. The other two programmable parameters of the flashlamp i.e., pulse duration and frequency were fixed at 2.5 ms and 90 Hz respectively. The temperature was monitored and measured in-situ during the specimen manufacturing using an Optris PI640 thermal camera which was calibrated at 270 °C to ± 5 °C at this temperature. It was assumed that the emissivity value does not change significantly for higher temperatures [7] and therefore, the measured emissivity value of 0.875 was used for the experimentation.

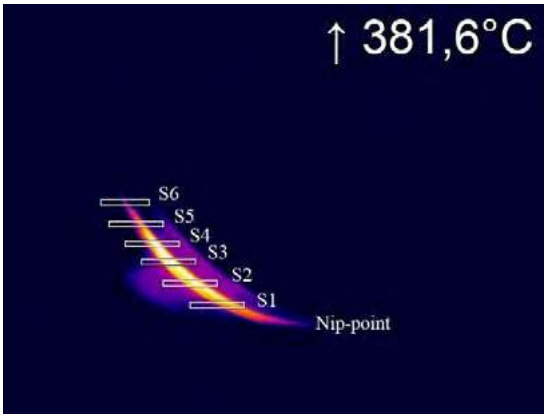

Figure 2. Thermal camera image captured during manufacturing.

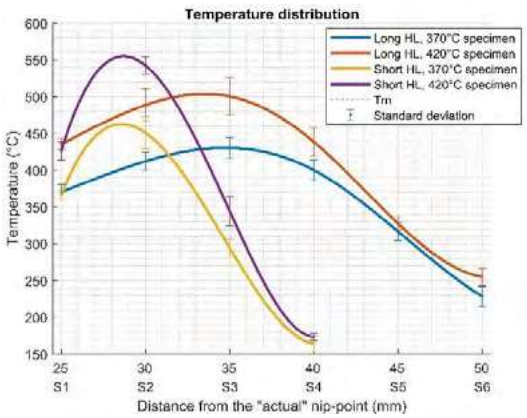

Figure 3. Temperature distribution along the heated length of the tape.

Figure 2 shows a thermal camera image captured while manufacturing the specimens. Several rectangular measuring bars that recorded the maximum temperature in it were placed at an approximate interval of 5 mm from each other with the closest one (S1) being approximately 25 mm away from the "actual" nip-point which is the first point of contact between the roller and the incoming tape. However, this point (S1) was considered to be the "visible" nip-point and used for the reference nip-point temperature for the experimental study as it was observed that the temperature started to drop after this

point due to the radiation being blocked by the geometry of the roller. Additionally, it was not reliable to measure the temperature closer to the nip-point than this point due to a large viewing angle between the tape and the view of the thermal camera and reflections from the layup tool. Another point to be noted is that the temperature distribution along the heated length of the incoming tape was not uniform. This is because the light guide's edge was at different distances to the incoming tape (light guide edge tangential to the roller). The temperature distribution trend along the heated length is shown in **Figure 3**. The specimens that reached a temperature of up to 560 °C were deemed viable for the experimental study as it did not show any abnormalities in surface roughness data and the cross-section view for any signs of a burnt resin.

2.2.3. Heated length

The Heated Length (HL) in this study is defined to be the length of the incoming tape that is heated above the T_g during the manufacturing in addition to the shadow zone (between actual and visible nip-points). For long HL, the longer edge of the light guide was used to expose a longer tape length to the broadband radiation while for short HL, the shorter edge of the light guide was used along with a metallic tape guiding plate that blocked some length of the incoming tape from being irradiated by the flashlamp.

The heated length was monitored during the specimen manufacturing by the temperature measuring bars (as shown in **Figure 2**) which were placed at known approximate distance from each other. Therefore, the length measured were 35-40 mm for the short HL specimens and 45-50 mm for the long HL specimens with an exception for the specimens at 250 °C and 300 °C with a heated length of 30 mm and 35 mm respectively because of the lower temperatures.

2.3. Tape Width Measurement

An image of certain length of the tape surface was captured using the microscope camera and was then processed in MATLAB to obtain the width measurement data. The image processing involved converting the grayscale image into a binary image by taking the grayscale value that occurred the least number of times in the image as the threshold to distinguish between the tape and the background. This was then followed by converting the binary image into a digital tape with clear tape edges to extract the width data.

For the as-received tape, 10 images scanning a length of 15.4 mm each for width measurement were taken approximately at every 1 m of the spool which was then used to manufacture all the specimens. For the post-process tape, two images scanning a length of 70 mm each for width measurement were taken for each specimen.

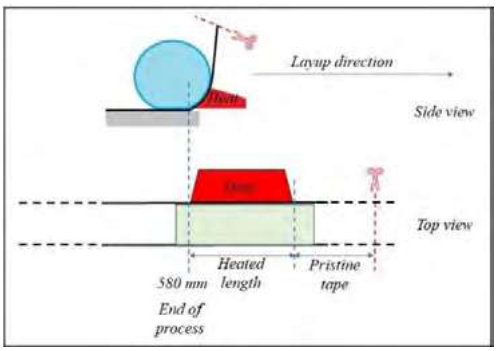

Figure 4. Tape after end of process and scanned area (in green) for width data in heating phase.

To check the width of the tape in the heated zone i.e., the heating phase of the process, the tape surface image was taken at the location highlighted in green in **Figure 4**, which schematically illustrates the tape after the end of the process. The length of the tape marked as the heated length very well represents the heating phase during the process as it was still heated after the end of the process without being consolidated by the roller. This allowed the inspection of the tape before compaction with all the other

boundary conditions of the process such as roller compaction pressure on one side and tape under tension from the other side.

2.4. Post-processing Microscopy

For all the post-processing microscopy experiments i.e., roughness analysis, tape cross-section profile and edge inspection, the Keyence VK-X1000 Laser Scanning Confocal Microscope (LSCM) was used with a built-in software for roughness analysis. ISO-4287 standard was followed for the roughness measurement and images were captures at 2.5X and 20X magnification for tape cross-section profile and edge inspection respectively.

3. Results and Discussion

3.1. Characterization and investigation of tape width deformation mechanism

Figure 5 shows a typical post-processed tape inspection in the heating zone as described in **Figure 4**. It is clearly seen from the digital tape in **Figure 5a** that the tape width deforms in the entire heating zone i.e., the heating phase of the process. However, further looking at the width data in **Figure 5b**, it was seen that the deformation follows a unique pattern. This has been illustrated in **Figure 6** where L_h, L_c, W_i, W_f are the heated length, contact length under roller, initial tape width and final tape width respectively. For further analysis, the width data graphs were divided into 5 different zones manually and a linear curve was fitted through each of the zones. Note that the data had some outliers in the form of sudden spikes because of detection of some loose fibers or particles in the image processing.

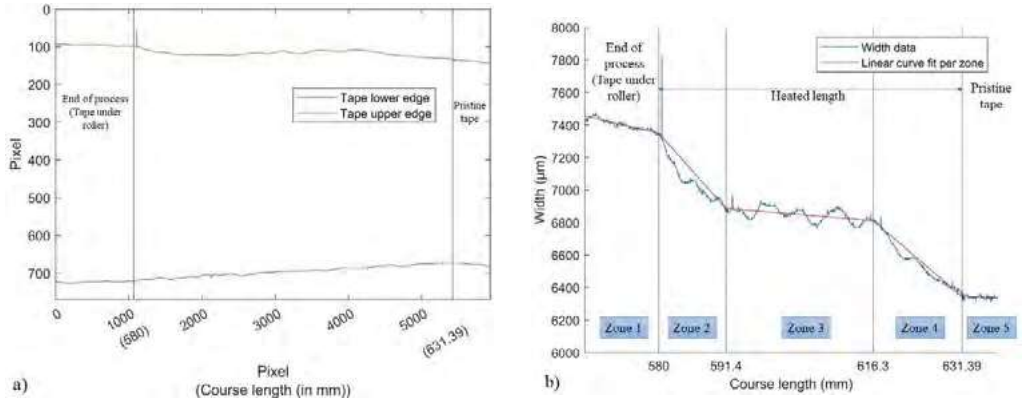

Figure 5. Tape profile inspection in heating phase: a) Digital tape b) Width data with zone divisions

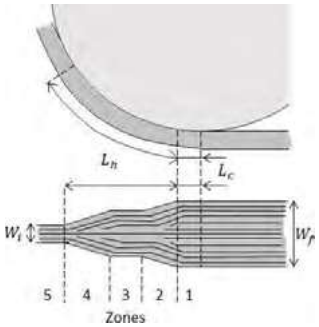

Figure 6. Tape width deformation as observed from results.

Zones 2, 3 and 4 represent the heated length during the process. It can be seen that zones 2 and 4 have a clear slope in the width deformation data whereas, zone 3 shows a flat plateau-like region. The slope in zone 2 suggests that there is width deformation due to the roller compaction in zone 1 and therefore the tape further widens before the nip-point i.e., in zone 2. Referring to the temperature distribution curves along the heated length of the tape as shown in **Figure 3**, it is clear that not the entire heated

length is heated above the T_m. Therefore, using this information, the slope in zone 4 is explained to be an indication of the tape below the T_m as the tape is not in the melt state completely and is therefore restricted in the width deformation due to the restricted movement of the polymer (resin) chains below the T_m. And, the plateau in zone 3 is an indication of the tape that is completely in the melt state and therefore, can deform freely.

The horizontal length data of zone 2 for all 3 samples of each specimen configuration, shown in **Figure 7**, was extracted from the curve fits and analyzed. It can be observed that there is a clear difference in the average horizontal length for the 300 N and 900 N configurations (5.22 mm for L/300 (excluding the outlier for L/300/420) and 12.57 mm for L/900 configurations). This increase in the horizontal length at zone 2 with increasing compaction force further confirms the dependence of zone 2 on the roller compaction force. Furthermore, it can be seen that the average horizontal length also increases with increase in temperature for all the configurations as shown by the trend lines in blue. This temperature dependence indicates that for the 370 °C configuration specimens, there is still some restricted movement of the polymer chains. Referring again to the temperature distribution curves along the heated length of the tape in **Figure 3**, it can be seen that the temperature was measured approximately 25 mm away from the "actual" nip-point and therefore it is highly likely that the tape temperature for the 370 °C configuration specimens dropped below the T_m because of the apparent shadow zone. For the 420 °C specimens, it is more likely that the tape remained above the T_m and therefore less restricted movement of the polymer chains resulting in larger length of the tape deforming at the same compaction pressure.

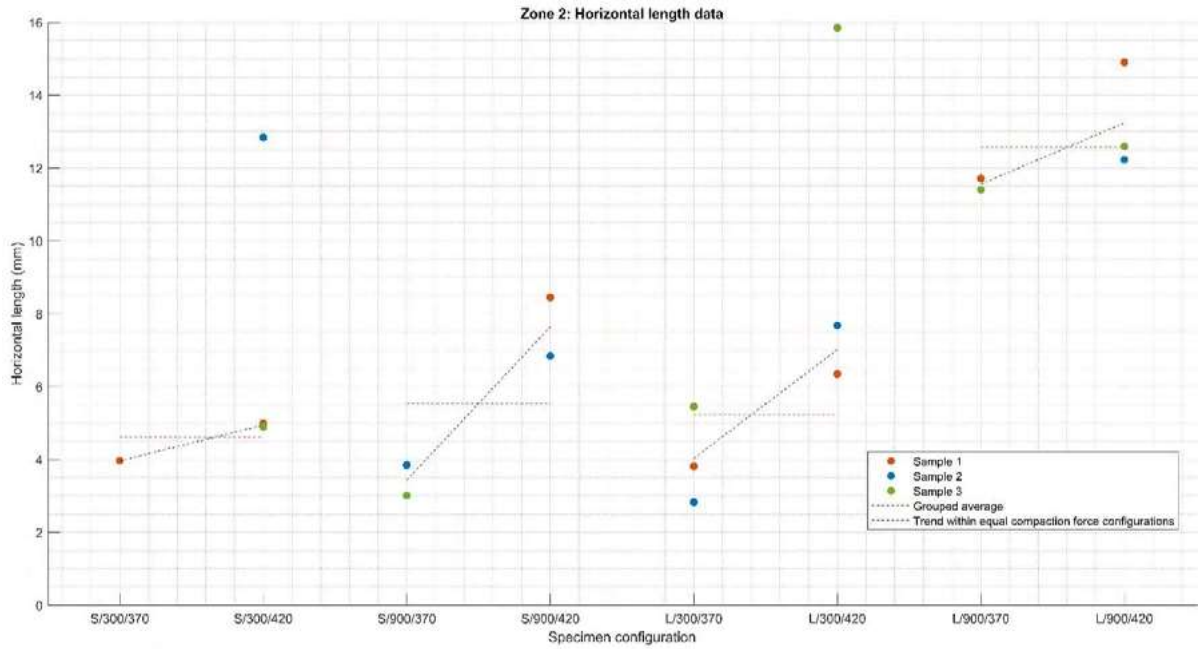

Figure 7. Zone 2 horizontal length data of all specimens. (Specimen Nomenclature: Heated length/Compaction Force/Temperature)

The surface roughness results show that the roughness remains almost the same as the as-received tape for the long HL and higher temperature configuration specimens, indicating that the temperature distribution might have an influence on the roughness value as the material would be able to flow more easily and consolidate more uniformly when the tape is more uniformly heated with larger part of the tape (both in length and thickness direction) in the melt state. This would therefore result in lower roughness. **Figure 8** shows the decrease in roughness with increase in processing temperature for short HL and 900 N compaction force specimens, including the extra temperature data point specimen at 300 °C. A linear decrease in the average R_q value is clearly observed from the plot.

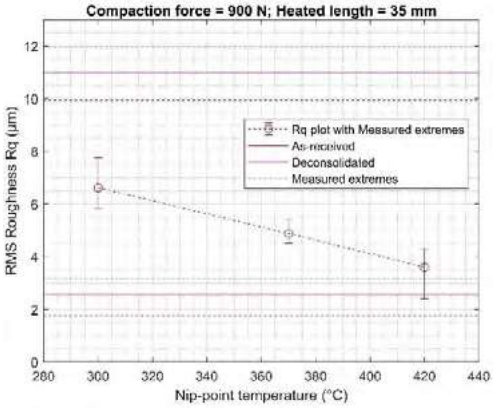

Figure 8. RMS Roughness R_q values over nip-point temperature for 900 N compaction force and short HL specimens.

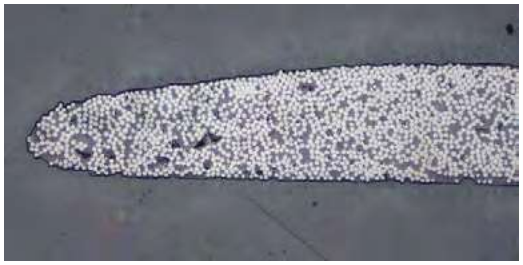

Figure 9. Typical tape cross-section view at the edge after processing.

The tape cross-section in general shows a thickness slope at the edges of the tape, as seen in **Figure 9**, compared to the rectangular edges for the as-received or deconsolidated tapes. This gradual reduction in the thickness around the tape edges is believed to be because of the compaction under the roller i.e., in the consolidation phase of the process. The tape under the roller takes the shape of the transitioning shape of the conformable roller at the edges as the tape is in the melt phase and can easily deform. Additionally, the edge inspection shows the presence of both fibers and resin (clearly visible in **Figure 9**). Therefore, this indicates that the width deformation involves spreading of the fiber-resin mixture.

3.2. Influence of processing parameters on the tape width

Figure 10a shows the width data over the heated length for the 300 N compaction force specimens and the two nip-point temperatures of 370 °C and 420 °C are plotted. The influence of longer heated length is directly associated with two factors, i.e., larger length of the tape being in the melt phase and more heating time. These factors are assumed to promote better heat distribution in the length and thickness direction of the tape and thereby promote the spreading of the fiber-resin mixture due to less restricted movement of the polymer chains in zones 2, 3 and 4 i.e., the heated length of the tape as described in **Figure 5**. However, this can only be seen clearly in the results for the specimens at 370 °C nip-point temperature. For the 420 °C configuration specimens, it is assumed that the higher temperature will itself promote better heat propagation through the thickness of the tape and therefore overshadow the effect of the longer heated length.

Figure 10b shows the width data over the nip-point temperature for short HL configuration and the two compaction forces of 300 N and 900 N are plotted. Width data for the specimens below the T_m i.e., at 250 °C is also plotted and it can be seen that the width deformation already takes place below the T_m. An average increase of up to 6.87% for the 900 N compaction force specimen is observed. The effect of processing temperature is directly related to the melt viscosity and polymer chain movement. As the temperature increases, the melt viscosity of the resin decreases along with less restrictions in the movement of the polymer chains which would thereby promote the spreading of the fiber-resin mixture. This can be seen clearly from the results where the width increases with increase in temperature. Again, additional width deformation due to the higher compaction force is believed to be the reason for the overlap in data for the two temperatures above the T_m.

Figure 10c shows the width data over the compaction force for the short HL specimens and the different nip-point temperatures are plotted. Previous results show that the width deformation takes place due to the spreading of the fiber-resin mixture. Therefore, the effect of the compaction pressure is directly dependant on the melt viscosity of the resin and the strain of the fibers. For the short HL configuration, the specimens at 370 °C shows an increase in width with compaction force which means that there is some restricted movement of the polymer chains at this temperature and therefore, increasing the

compaction force helps in the flow of the polymer chains and thereby increases the width. For the specimens at 420 °C, the spreading remains the same with increase in compaction force indicating that either a very low melt viscosity or the maximum strain of the fibers is achieved.

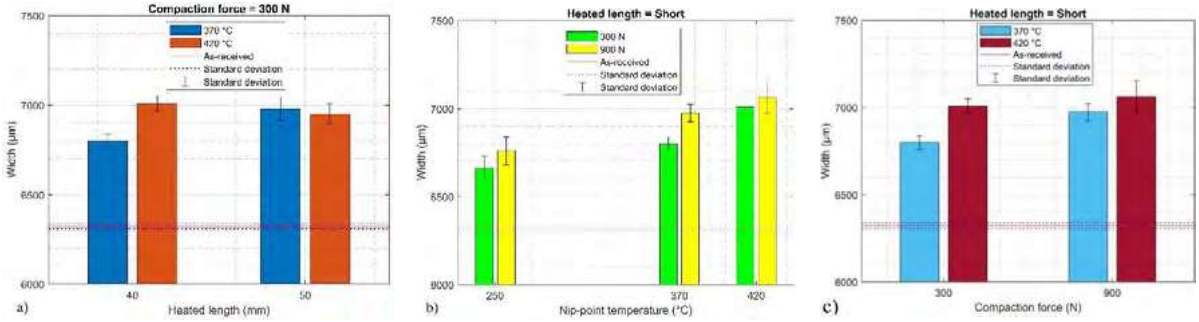

Figure 10. Tape width values over: a) heated length b) nip-point temperature and c) compaction force.

4. Conclusion and Future work

The results obtained in this study provide a better understanding of the tape width deformation of thermoplastic prepreg tapes by in-situ AFP processing. Width deformation involves the spreading of the fiber-resin mixture in the consolidation as well as the heating phase of the process. Moreover, the tape deformation profile shows a gradually decreasing thickness on the edges. The process parameter settings promoting a uniform temperature distribution in both the length and thickness direction of the tape i.e., longer heated length and higher temperature, in general stabilizes the surface roughness and width deformation. For future work, the influence of other processing parameters and boundary conditions such as placement speed and roller hardness should be inspected. Finally, these results should be incorporated into the current AFP processing models to accurately predict the tape width deformation and therefore, mitigate the problem of gaps and overlaps.

References

[1] M. J. Donough et al. “Process modelling of In-situ consolidated thermoplastic composite by automated fibre placement – A review”. In: *Composites Part A: Applied Science and Manufacturing* 163 (2022), p. 107179. issn: 1359-835X. doi: https://doi. org/10.1016/j.compositesa.2022.107179.

[2] F. Heinecke and C. Willberg. “Manufacturing-Induced Imperfections in Composite Parts Manufactured via Automated Fiber Placement”. In: *Journal of Composites Science* 3.2 (2019). issn: 2504-477X. doi: 10 . 3390 / jcs3020056.

[3] T. Kok. “On the consolidation quality in laser assisted fiber placement: The role of the heating phase”. PhD thesis. Netherlands: *University of Twente*, 2018. isbn: 978-90- 365-4606-5. doi: 10.3990/1.9789036546065.

[4] N. Yadav and R. Schledjewski. “Inline tape width control for thermoplastic automated tape layup”. In: *Composites Part A: Applied Science and Manufacturing* 163 (2022), p. 107267. issn: 1359-835X. doi: https://doi.org/10.1016/j.compositesa. 2022 . 107267.

[5] M. A. Khan. “Experimental and Simulative Description of the Thermoplastic Tape Placement Process with Online Consolidation”. PhD thesis. *Technische Universität Kaiserslautern*, 2017. url: http://nbn-resolving.de/urn:nbn:de:hbz: 386-kluedo-47293

[6] J. Jiang et al. “Pressure distribution for automated fiber placement and design optimization of compaction rollers”. In: *Journal of Reinforced Plastics and Composites* 38.18 (2019), pp. 860–870. doi: 10.1177/0731684419850896.

[7] X. Li and W. Strieder. “Emissivity of High-Temperature Fiber Composites”. In: *Industrial & Engineering Chemistry Research* 48.4 (2009), pp. 2236–2244. doi: 10.1021/ie8008583.